参考資料

TI Designs: TIDA-01598
ソーラー・インバータ用のローサイド、高帯域幅電流増幅およびエラー検出のリファレンス・デザイン

概要

このリファレンス・デザインは、フォルト検出機能が内蔵された、ローサイドの正確なシャントベースの電流測定用ソリューションです。高帯域の電流センシングをサポートする電流センス・アンプで構成されます。フォルト検出機能により、低電流および過電流フォルトを検出できます。このデザインでは、シャント・ベースの電流センシングと、ホール・センサを使用する電流センシングとの間の性能比較が可能です。

リソース

TIDA-01598	デザイン・フォルダ
INA240	プロダクト・フォルダ
LMV393-N	プロダクト・フォルダ
TLV431	プロダクト・フォルダ
OPA350	プロダクト・フォルダ
SN74LVC1G17	プロダクト・フォルダ
TPS717	プロダクト・フォルダ
LP2985	プロダクト・フォルダ
TLV760	プロダクト・フォルダ

TI E2E™ Community

E2E™エキスパートに質問

特長

- 負の同相をサポートする、シャント・ベースのローサイド電流センシング・システム
- 電流センシング用の小型システム
- 400kHzまでの高帯域電流センシング
- 双方向電流センシングのサポート
- 低電流および過電流検出機能が内蔵されており、応答時間は1µs以内
- DC電流範囲(-3A～15A)の全体にわたって測定誤差0.3%未満
- レベル・シフト出力用に0.62 V_{REF}を内蔵

アプリケーション

- 太陽光ストリング・インバータ
- 太陽光中央インバータ

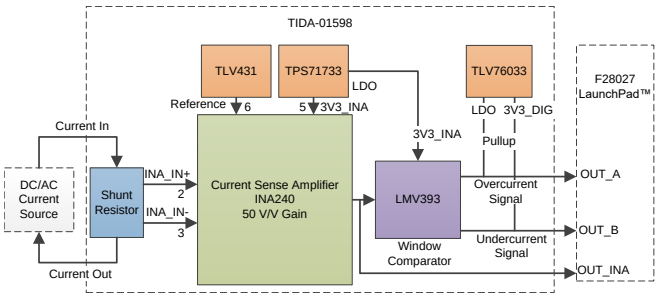

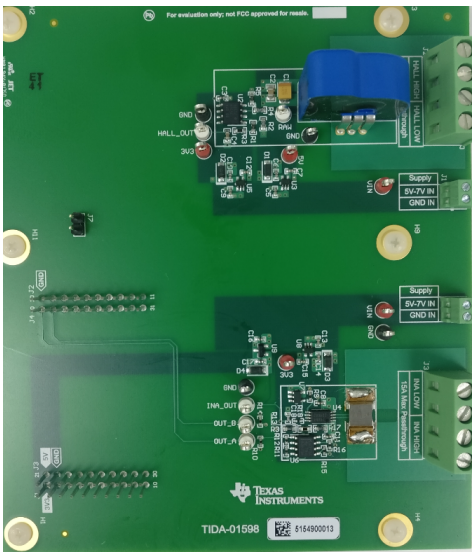

1 System Description

Solar panels consist of photovoltaic solar cells which harvest solar energy from the sun and generate electricity. The DC current and voltages generated in solar panels is then converted to AC to be fed in the grid. A string inverter is connected to multiple solar panels in series for this purpose. The current range generated by the panel typically varies from 12 A to 15 A. It is necessary to monitor this current to effectively operate the DC/DC MPPT input of the solar inverter. Additionally, in case of an overcurrent fault, the current exceeds the maximum current limit and thus can damage the power devices in the inverter. Reverse current faults where the current flows into the panels can damage the solar panels. Overcurrent and reverse current faults must be detected and resolved quickly.

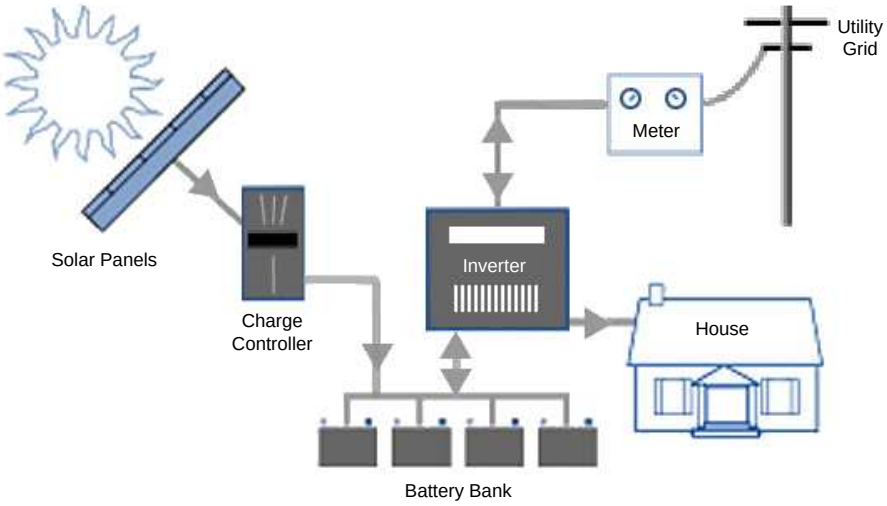

図 1. Typical Solar System

1.1 Current Monitoring

Current monitoring methods include high-side sensing and low-side sensing. In high-side sensing, the current-sensing element is connected between the supply and the load whereas in low-side sensing, the current sensing element is connected between the load and ground.

1.1.1 Hall Sensors

Closed-loop current transducers use a ferro-magnetic core with a sensing element or field probe inserted into a gap in the core. The core picks up the magnetic field created by the current flowing through the primary winding. Changes in the magnetic field are measured by the sense element and are passed on to a signal conditioning stage for filtering and amplification. The coil driver stage provides current to the compensation coil which creates an opposing magnetic field that cancels the effect of the primary current. The compensation current passes through a shunt resistor which provides a differential voltage to a precision sense amplifier. The amplifier gains the shunt voltage and drives the output stage of the transducer. The resulting voltage output is proportional to the current flowing through the primary winding as shown in the transfer function defined in Equation 1. Additional amplification and scaling can be done before the signal reaches a system ADC.

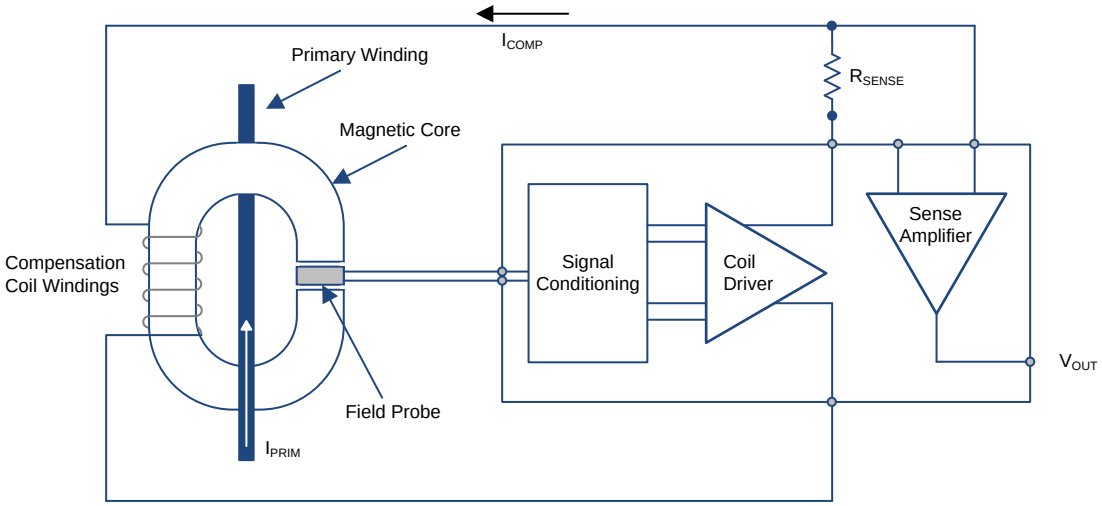

図 2. Closed-Loop Sensor Block Diagram

$$V_{OUT} = I_{PRIM} \times \left(\frac{N_P}{N_S}\right) \times R_{SENSE} \times Gain \quad (1)$$

By nature of the separation of the primary current carrier and the magnetic flux concentration coils, the Hall-effect sensor is inherently isolated. The physical limits of the sensor limit the overall total bandwidth to typically < 200 kHz. Additionally, the added complexity also increases cost versus other sensor solutions. For the TIDA-01598, an LEM LTS 15-NP Hall-effect sensor was placed beside the shunt-based solution to provide a direct comparison.

1.1.2 Shunt Sensors

Current sensing can be done by measuring the voltage drop across a shunt resistor. On the high side, current can be monitored directly from the source with immunity to ground disturbances. The common-mode range of the amplifier has to include the supply voltage which may exceed the supply voltage range, thus requiring isolation. Alternatively, low-side sensing can be used for which the common-mode voltage is zero.

Compared to magnetic-based sensing solutions, shunt sensors are very simple transducers capable of measuring a wide bandwidth current signal. However, they do lack the inherent galvanic isolation that comes with using a Hall sensor. Shunt sensors could also introduce undesired power loss in the system due to the voltage drop across the sensor. This power loss is dissipated as heat in the system, which could also influence nearby components negatively. Care must be taken to ensure that the power loss is minimized.

1.2 Low-Side Current Sensing

The low-side current-sensing module consists of the following subsystems:

1.2.1 Current Sensor

To read current, measure the voltage drop across a shunt resistor. Shunt resistors have a very low resistance value and cause a voltage drop of around 10 mV to 100 mV.

1.2.2 Signal Conditioning

A signal conditioning circuit is used to scale the low-voltage drop across the shunt element. The amplifier used for this purpose can be a precision op amp, instrumentation amplifier, programmable-gain amplifier, and a differential amplifier or isolation amplifier. The amplifier selection depends on the accuracy and temperature drift requirements. The TIDA-01598 uses a current sense amplifier with a fixed gain, high bandwidth, and also supports negative common-mode voltages.

1.2.3 Power Supply

The current-sensing module requires only an independent onboard supply ranging from 5 V to 6.5 V. Low dropout (LDO) regulators are used to provide a voltage supply to the current sense amplifier, comparator, Hall sensor, and scaling amplifier in the circuit.

表 1. TIDA-01598 LDOs

LDO REGULATOR	OUTPUT VOLTAGE	COMMENTS
TPS717	3.3 V	Scaling amplifier, window comparator supply voltage
TLV760	3.3 V (Digital)	Pullup voltage
LP2985	5 V	Hall-sensor supply voltage

1.2.4 Fault Current Detection

A fault detection circuit is used to detect overcurrent and negative current conditions. An arc can create faulty negative currents which must be detected. Dual comparators configured as window comparator circuit with low propagation delay can be used to generate voltage signals in case of a fault. The typical timing requirement of overcurrent and negative current fault detection is less than 2 µs. This design achieves a system fault-detection response time of less than 1µs.

1.3 Featured Applications

The section provides information on different end equipment where low-side, high-bandwidth current amplification and fault detection can be used

1.3.1 Solar Inverters

Solar inverters are necessary for converting the DC voltage and currents generated by the solar panels to AC voltage and currents to feed in the grid. It is necessary to monitor current for efficiency and to protect sensitive devices. A shunt-based current-sensing device can be placed on the low side of each solar string and one at the common to effectively measure the current through each string of the solar string inverter. The output of the shunt sensor can then be used as the control algorithm input by a processing unit.

In an inverter with (N) solar string inputs, a TI design consisting of (N + 1) shunt-based sensors has a lower cost than (N) Hall sensors placed on the high side and shows better performance in terms of accuracy in current measurement, high-bandwidth sensing, and solution size. The TI design solution finds a similar application in solar central inverters.

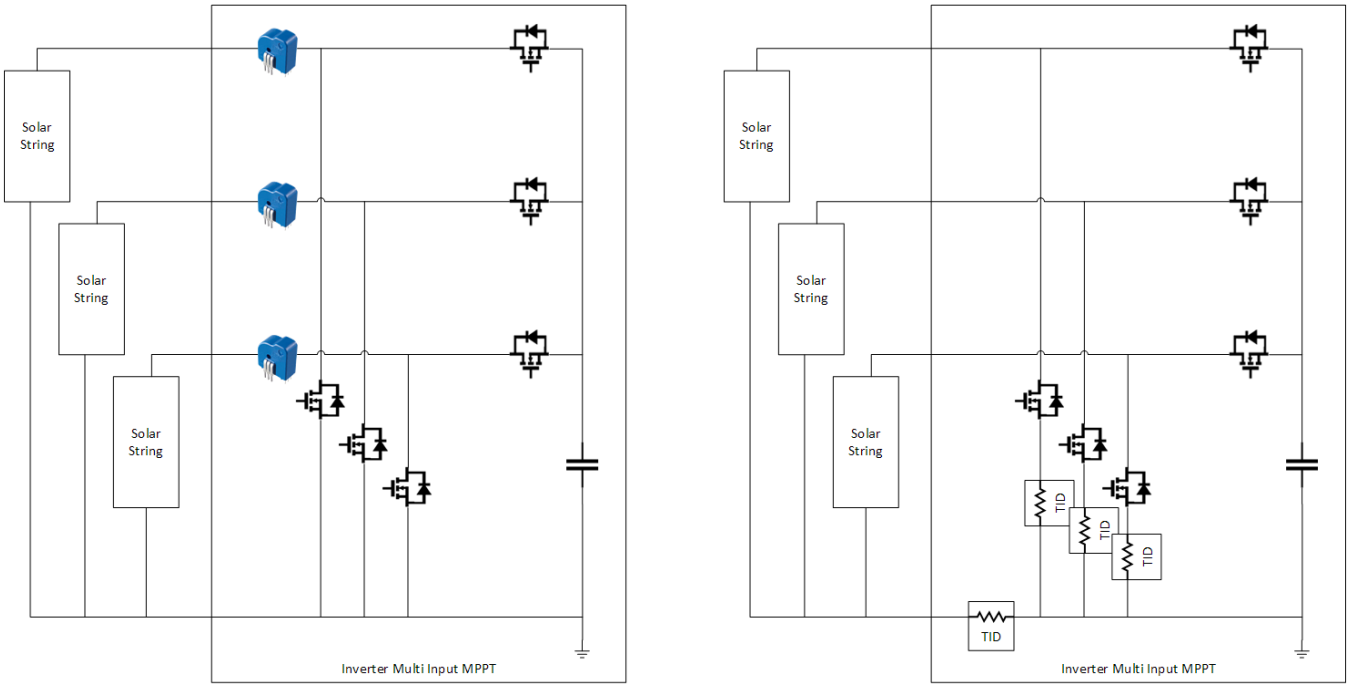

図 3. Current-Sensing Solution for a Solar Inverter Application Using a) Hall Sensors on High Side and b) Shunt-Based Low-Side Sensing

1.4 TI Design TIDA-01598 Advantages

This TI Design using a current sense amplifier with a fault detection circuit provides the following advantages over the design using Hall effect based sensors:

- Higher bandwidth sensing of up to 400 kHz is possible
- Smaller solution footprint
- Provides for an integrated overcurrent and undercurrent detection
- Provides a lower noise floor

- Reduced total solution cost

1.5 Key System Specifications

表 2 shows key specifications provided by shunt-based current measurement.

表 2. Key System Specifications

PARAMETER	DESCRIPTION	COMMENTS
Current measurement range	Up to 15-A DC current	Up to 3-A negative current can be measured in case of a reverse current fault
Measurement accuracy	Less than 0.05% for the complete current range.	
AFE bandwidth	High-bandwidth sensing of up to 400 kHz	
Current shunt	Shunt resistor with low resistance and low temperature coefficient value	Equivalent shunt resistance formed by connecting two resistors in parallel to increase current carrying capacity and reduce potential critical faults if a shunt fails.
Amplifier	50 V/V fixed gain, current sense amplifier	With adjustable reference voltage to vary current range in the positive or negative direction
Power supply	Onboard supply and LDO regulators	Low noise (30 μV_{RMS})
Window comparator	Dual comparator with a low propagation and resistive network to detect fault	According to overcurrent and undercurrent specifications
Dual comparator bandwidth	High-bandwidth support of up to 500 kHz	
Reference	Voltage shunt regulator to provide constant reference voltage to the current sense amplifier	According to the current-sensing range requirement in either direction

2 System Overview

2.1 Block Diagram

This TI design TIDA-01598 showcases the following configuration for system performance comparison between:

- Current sense amplifier INA240 with fault detection
- Hall effect based current transducer with signal conditioning

2.1.1 Current-Sense Amplifier INA240 With Fault Detection

The current-sense amplifier INA240, with fault detection, has the following functional blocks:

- Current sense amplifier INA240 with 50 V/V gain to measure the voltage drop across the shunt resistor.
- Voltage shunt regulator to provide constant reference voltage to the INA240.
- LDO regulators to generate the required power supply.
- High-speed window comparator to detect overcurrent and undercurrent fault.

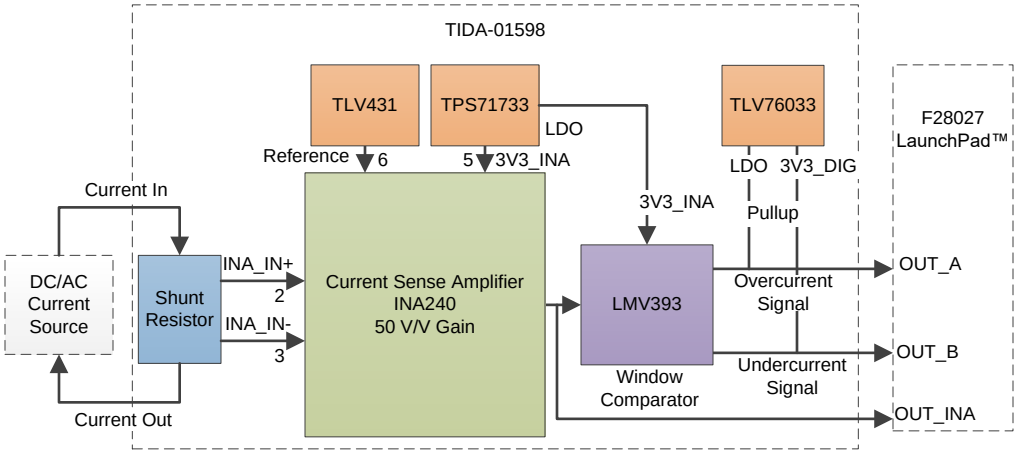

図 4. TIDA-01598 Shunt Block Diagram

2.1.2 Hall Effect Based Current Transducer With Signal Conditioning

The Hall effect based current transducer with signal conditioning has the following functional blocks:

- Hall effect based current transducer to sense current up to 15 A
- Low noise, LDOs to generate the required analog and digital power supply.
- Scaling op amp to scale the output of a Hall sensor according to the ADC input range.

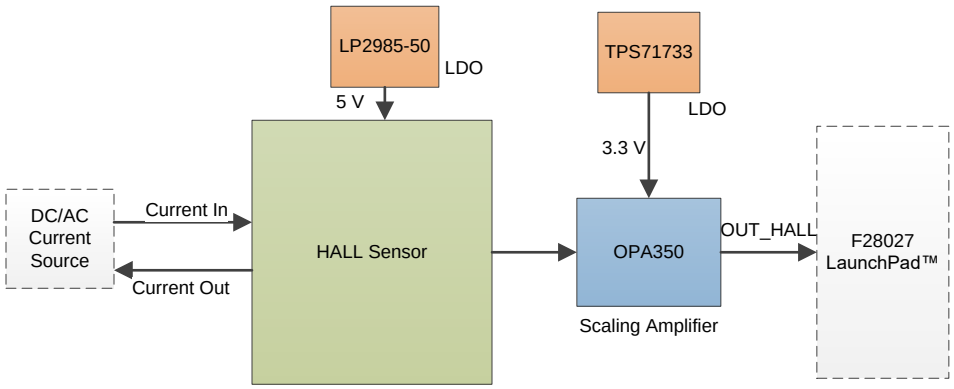

図 5. TIDA-01598 Hall Sensor Block Diagram

2.2 Highlighted Products

This section provides details on the TI products used in this TI design.

2.2.1 Bidirectional Current Sense Amplifier

2.2.1.1 INA240

The INA240 device is a bidirectional current sense amplifier with a wide common-mode range, zero drift topology, enhanced PWM rejection, and excellent CMRR. The device family offers four fixed gain values: 20 V/V, 50 V/V, 100 V/V and 500 V/V, and a high-gain accuracy with gain error less than 0.2% and low offset value allowing sensing of minimum a voltage drop as low as 10 mV. The reference voltage input of the device allows for both a positive and negative current range, according to requirement. For more information, see the INA240 product page.

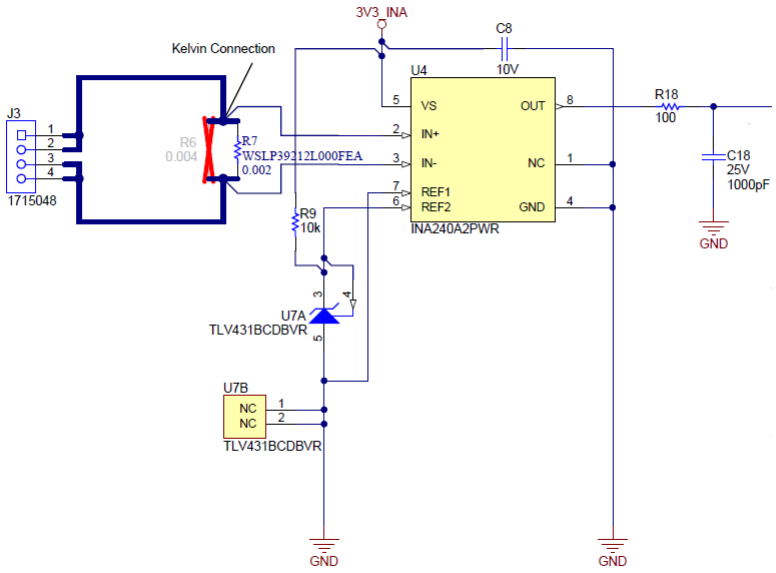

図 6. INA240 Connections

2.2.1.2 LMV393

The LMV393 device is a low-voltage and low-power dual-differential comparator with an open collector output and a low propagation time delay of 0.2 µs. For more information, see the LMV393 product page.

2.2.1.3 SN74LVC1G17

The SN74LVC1G17 device is a single Schmitt-trigger buffer with a low propagation delay of 4.6 ns at 3.3-V supply operation which maintains low static power dissipation. For more information, see the SN74LVC1G17 product page.

2.2.1.4 TPS717

The TPS717 is a family of LDO linear regulators with an output voltage ranging from 0.9 V to 6.2 V. The device family offers a high power-supply rejection ratio and very low dropout of 170 mV at 150 mA, and display very low noise of 30 μV_{RMS} (100 Hz to 100 kHz). For more information, see the TPS717 product page.

2.2.1.5 TLV760

The TLV760 device is a fixed output linear voltage regulator with a wide input voltage range of up to 30 V, available in a small size 3-pin SOT-23 packaging. The TLV760xx is available 3.3-V, 5-V, 12-V, and 15-V output voltage versions. For more information, see the TLV760 product page.

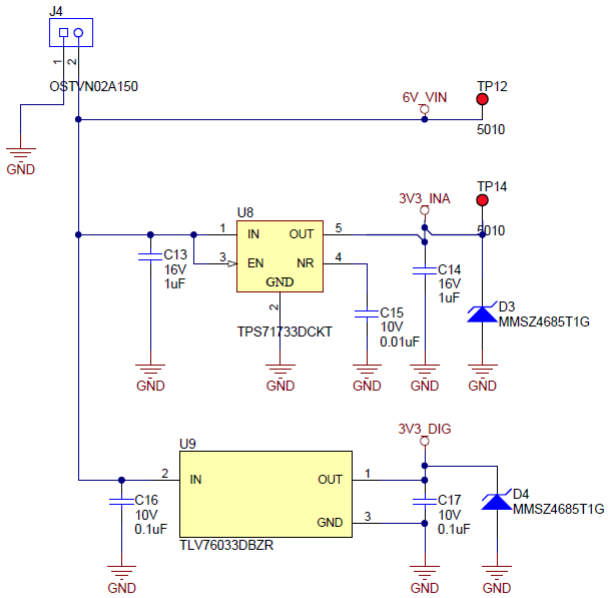

図 7. Analog and Digital Power Supply

2.2.1.6 LP2985

The LP2985 is a family of low noise and LDO regulators with 150-mA continuous load current and output voltage tolerance of 1%. It has overcurrent and overtemperature protection features. For more information, see the LP2985 product page.

2.2.1.7 TLV431

The TLV431 device is a low-voltage adjustable precision shunt regulator with adjustable output, ranging from 1.24 V to 6 V. The TLV431x family offers reference voltage tolerances of 0.5%, 1%, and 1.5%. For more information, see the TLV431 product page.

2.2.2 Design Enhancements

The following section provides some of the design enhancement options:

2.2.2.1 Shunt Resistor Selection and Sizing

The shunt resistor selection depends on the available supply voltage, full-scale current to be measured, and the current sense amplifier device gain. A minimum resistor can be chosen to maximize the current input range of the circuitry.

Shunt resistor size affects the current measurement accuracy and power dissipation across the resistor. A larger resistor improves the current measurement accuracy of the circuitry but also leads to increased power dissipation across the resistor. The heat generated due to the power dissipation may adversely affect the current measurement accuracy of the resistor due to the resistor temperature coefficient. Thus, this TI Design (TIDA-01598) uses a current shunt resistor with a temperature coefficient as low as ±75 ppm/°C. Current sense amplifiers with higher gain are required if smaller shunt resistors are used which lead to increased error and noise parameters. This TI Design uses the INA240 device which maintains a high-performance level for higher gain settings.

表 3 shows the steps for selection of shunt resistors for INA240 with 3.3-V supply voltage and current-sensing range of up to 15 A.

表 3. INA240 Shunt Resistors

PARAMETER	EQUATION	RESULTS
INA240 output range	V_{GND} + 1 mV < V_{OUT} < VS – 0.05 V	1 mV < V_{OUT} < 3.25 V
Gain	-	50 V/V (INA240A2)
INA240 input range	V_{IN} = (V_{OUT}) / 50	20 µV < V_{OUT} < 0.065 V
Current range	-	0.25 A < I_{LOAD} < 15 A
$R_{SHUNT-MAX}$	V_{IN-MAX} / $I_{LOAD-MAX}$	4.3 mΩ
$R_{SHUNT-MIN}$	V_{IN-MIN} / $I_{LOAD-MIN}$	80 µΩ

As resistor power dissipation leads in self heating and system power losses, choose the largest R_{SHUNT} that the system can tolerate.

2.2.2.2 Bidirectional Input Current Range

The INA240 reference can be configured to alter the bidirectional current ranges to be sensed. The device reference pins can be connected together to the positive rail for maximizing negative input current to be measured and to the negative rail for maximizing positive input current to be measured. The reference pins can be connected to an external reference for an output of reference voltage for shorted inputs. The output voltage will increase over the reference voltage for positive current and decrease under the reference voltage for negative current. Connecting one reference pin to positive rail and the other to the negative rail will allow equal current in either direction. The current configuration with one pin connected to reference voltage of 1.24 V and another pin to ground allows for positive current measurement of up to 15 A.

2.2.2.3 Comparator With Low Propagation Delay

Choose a window comparator with low propagation delay for fault detection at high frequencies. The LMV393 device can detect fault accurately for frequencies up to 500 kHz. The TLV3202 and TLV3502 devices are dual high-speed comparators with low propagation delay which can be used for higher frequency fault detection requirement. 表 4 compares the propagation delay for these three parts.

表 4. Propagation Delay Comparison

COMPARATOR PART NUMBER	DESCRIPTION	PROPAGATION DELAY
TLV3202	Dual, microPower, rail-to-rail input comparator with push-pull outputs	47 ns
TLV3502	Dual, rail-to-rail input comparator with push-pull outputs	4.5 ns
LMV393	Dual general purpose low-voltage comparator	0.2 µs

3 Hardware, Software, Testing Requirements, and Test Results

3.1 Getting Started Hardware

This section describes the setup for testing the TIDA-01598.

3.1.1 Hardware

This section provides information on the different interface connectors for connecting the power supply and current input. 表 5 provides details on the different connectors used for applying the inputs and power supply for performance evaluation of the current sensing.

表 5. Connector Functions

CONNECTOR	FUNCTION	COMMENTS
J4	DC power supply to INA240	5-V to 7-V DC Supply
J1	DC power supply to Hall sensor	5-V to 7-V DC Supply
J3.1, J3.2	Input current IN to INA240	
J3.3, J3.4	Input current OUT to INA240	
J2.3, J2.4	Input current IN to Hall sensor	Current should not exceed 4.4 A_{RMS} and 25-A DC.
J2.1, J2.2	Input current OUT to Hall sensor	

3.1.2 Test Setup for Current Sensing

図 8 provides information on the setup used for current performance testing of the INA240-based current sense amplifier. The test setup for testing the TIDA-01598 consists of (1) DC power supply (–6 V), (2) TIDA-01598 TI design board, (3) AC current source, (4) DC source (10 V), (5) DC electronic load (programmable), (6) multimeter for measuring expected output voltage of the sensor.

注: While testing, make sure the inputs do not exceed the range specified in 表 5 for proper operation.

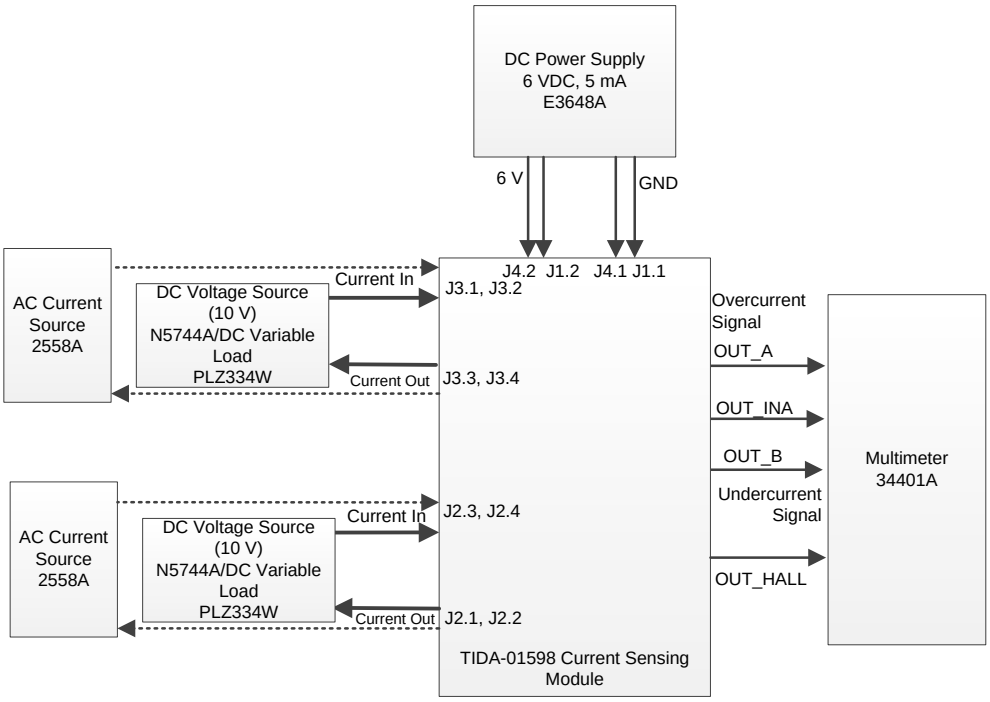

図 8. Setup for Testing Current Measurement Performance

3.2 Testing and Results

3.2.1 Simulation Results Using TINA-TI Software

The entire signal chain, including the INA240, LM393, TMS320C2x ADC input, and passive filters are simulated for AC transfer analysis and comparator response time using TINA-TI.

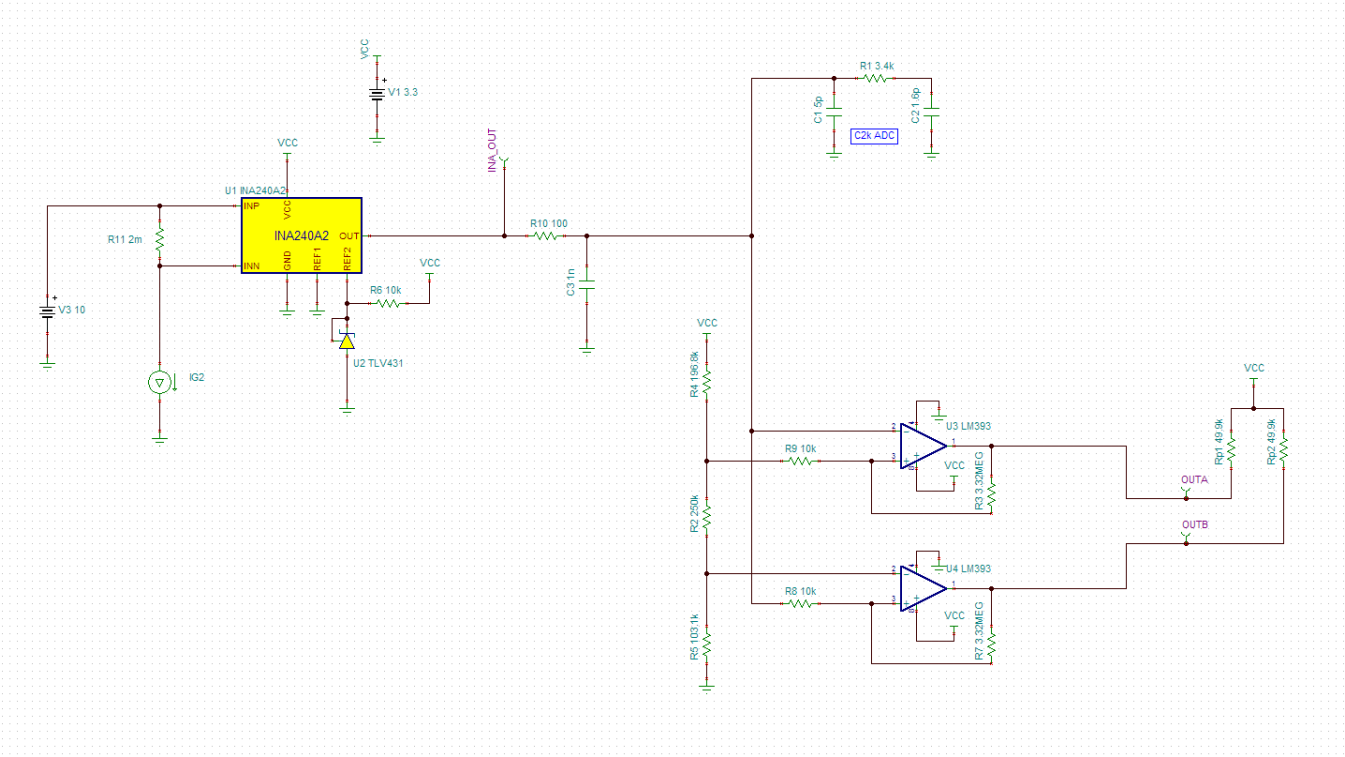

図 9. TIDA-01598 Simulation Model

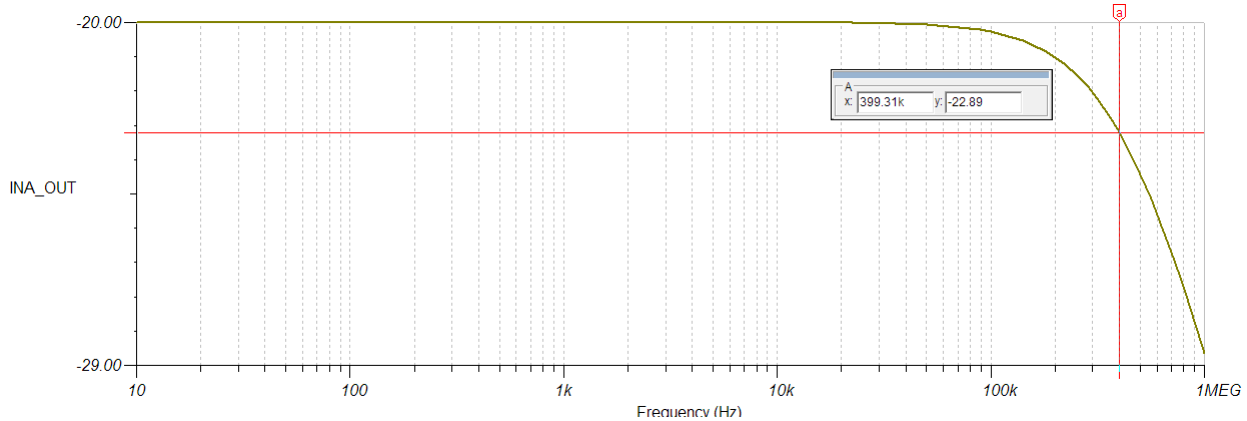

図 10. TIDA-01598 Frequency Response Simulation

Observe in 図 11 that the expected transfer of the analog current signal is still above the –3-db drop point at the target frequency of 400 kHz.

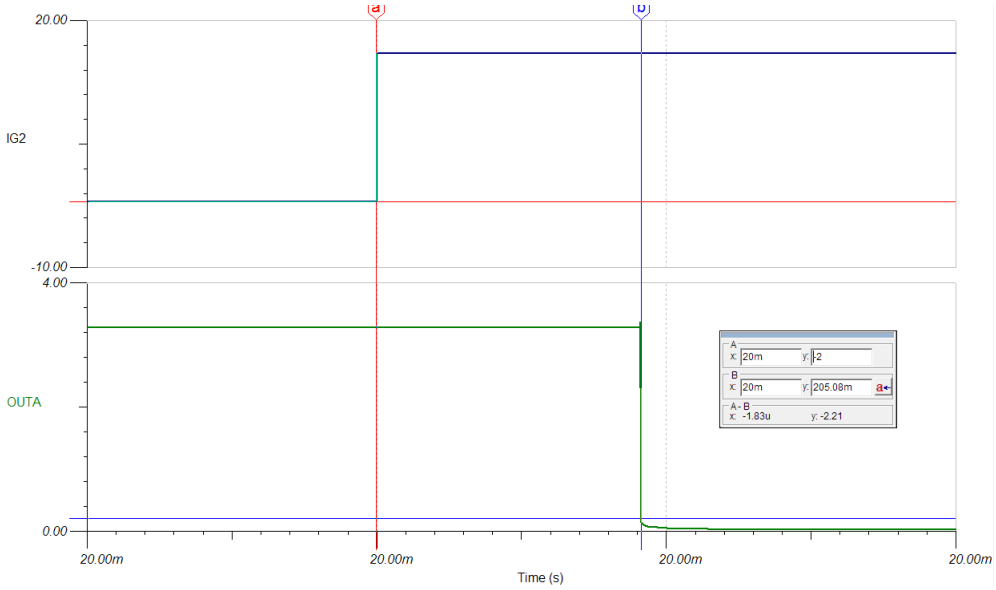

図 11. TIDA-01598 Overcurrent Response Simulation

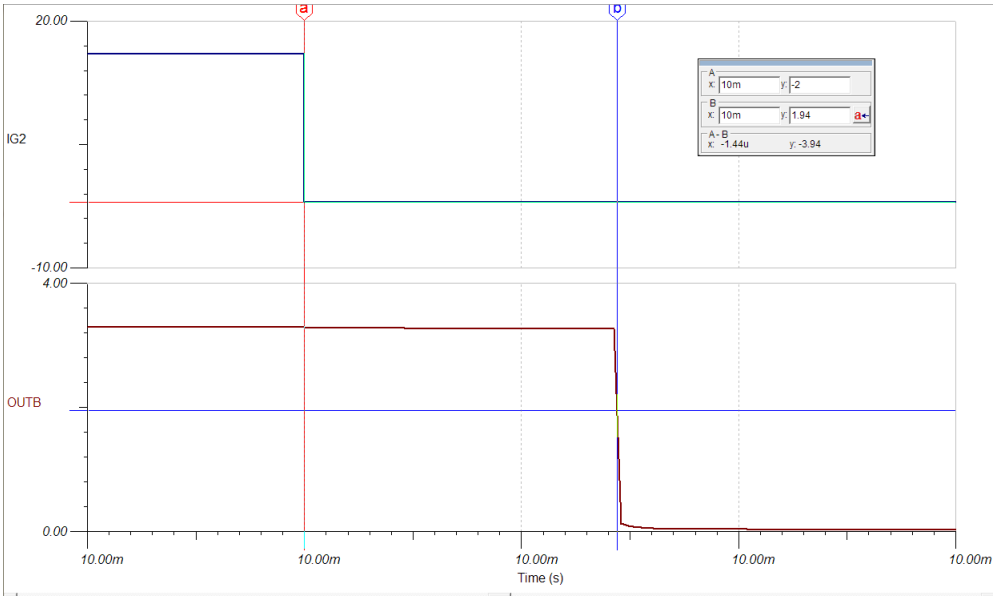

図 12. TIDA-01598 Undercurrent Response Simulation

To simulate an overcurrent and undercurrent event, a square current wave was pulsed through the shunt resistor that would force the event. The measured delay to the active-low system output was below the target of 2 µs.

3.2.2 Functional Testing

The following test conditions are provided for performance measurement.

The tests were done using a function generator or programmable current source or programmable DC voltage source and load. A multimeter was used to record output values.

表 6 provides details on the different functional tests that are done on the AIM.

表 6. Functional Tests on the AIM

PARAMETER	SPECIFICATION	MEASUREMENT
Observations for shunt-based current sensing:		
3.3-V LDO output	3.3 V	3.3 V
3.3-V DIG LDO output	3.3 V	3.28 V
INA240 current sense amplifier	Measurement of current functionality	OK
Window comparator	Detection of fault up to 400 kHz	OK
Shunt regulator for external Reference output	1.24 V	1.2433 V
Observations for Hall effect-based current sensing:		
5-V LDO output	5 V	4.98 V
3.3-V LDO output	3.3 V	3.3 V
HALL sensor-based current transducer	Measurement of current functionality	OK
Scaling amplifier	1.66 V/V Gain	1.66 V/V Gain

3.2.3 DC Current Measurement Performance Testing

This section provides details of the DC current measurement performance testing observations for DC current input varying from 0.25 A to 15 A. The output measured was averaged over 250 readings on a 34401A multimeter.

The current shunt resistor value is 3 mΩ.

表 7. Observation for Shunt-Based Current Sensing

CURRENT INPUT	INA240 EXPECTED OUTPUT	INA240 MEASURED OUTPUT	OUTPUT ERROR (%)
0.25 A	0.6575 V	0.6592 V	0.26%
0.5 A	0.6950 V	0.6969 V	0.27%
1 A	0.7700 V	0.7720 V	0.26%
1.5 A	0.8450 V	0.8475 V	0.29%
2 A	0.9200 V	0.9224 V	0.26%
3 A	1.0700 V	1.0730 V	0.28%
4 A	1.2200 V	1.2232 V	0.26%
5 A	1.3700 V	1.3737 V	0.27%
6 A	1.5200 V	1.5242 V	0.27%
7 A	1.6700 V	1.6741 V	0.25%
8 A	1.8200 V	1.8244 V	0.24%
9 A	1.9700 V	1.9751 V	0.26%
10 A	2.1200 V	2.1254 V	0.25%
12 A	2.4200 V	2.4260 V	0.25%
13 A	2.5700 V	2.5766 V	0.26%
14 A	2.7200 V	2.7271 V	0.26%
15 A	2.8700 V	2.8778 V	0.27%

The maximum error in the sensor output is 0.29% and the minimum error is 0.24%.

The variation of error in sensor output is 0.05% for the current range of 0.25 A to 15 A.

表 8. Observation for Hall Effect-Based Current Sensing

CURRENT INPUT	HALL EFFECT SENSOR EXPECTED OUTPUT	HALL EFFECT SENSOR MEASURED OUTPUT	OUTPUT ERROR (%)
0.25 A	2.5100 V	2.5124 V	0.08%
0.5 A	2.5210 V	2.5230 V	0.09%
1 A	2.5420 V	2.5440 V	0.09%
1.5 A	2.5630 V	2.5650 V	0.10%
2 A	2.5830 V	2.5860 V	0.10%
3 A	2.6250 V	2.6281 V	0.12%
4 A	2.6670 V	2.6700 V	0.13%
5 A	2.7080 V	2.7118 V	0.13%
6 A	2.7500 V	2.7539 V	0.14%
7 A	2.7920 V	2.7959 V	0.15%
8 A	2.8330 V	2.8380 V	0.16%
9 A	2.8750 V	2.8800 V	0.17%
10 A	2.9170 V	2.9219 V	0.18%
12 A	3.0000 V	3.0062 V	0.21%
13 A	3.0420 V	3.0481 V	0.21%
14 A	3.0830 V	3.0902 V	0.22%
15 A	3.1250 V	3.1322 V	0.23%

The maximum error in the Hall effect based sensor output is 0.23% and the minimum error is 0.08%. The variation of error in sensor output is 0.15% for (0.25 A–15 A) current range.

Shunt-based current sensing has lower error variation of 0.05% for DC current input whereas Hall effect based current sensing has a higher variation error variation of 0.15% for (0.25 A–15 A) current range. This TI design provides low cost and small size shunt-based current sensing with a lower error of 0.05% along with an integrated overcurrent and negative current fault detection feature.

3.2.4 AC Current Measurement Performance Testing

This section provides detailed observation of AC Current Measurement Performance testing for varying current inputs from 0.5 A RMS to 11 A RMS at 50 Hz, 60 Hz, and 400 Hz. The output voltage of the INA240 was set at 1.65 V at 0-V differential input by connecting one reference pin to ground and another to the supply voltage of the device (3.3 V) increasing the bidirectional current-sensing range of INA240 for testing purposes.

The current shunt resistor value is 2 mΩ.

表 9 and 表 10 show the test data observed at 50 Hz.:

表 9. Observation for Shunt-Based Current Sensing

INPUT CURRENT AT 50 Hz	INA240 EXPECTED OUTPUT	INA240 MEASURED OUTPUT	OUTPUT ERROR (%)
0.5 A	0.050 V	0.048 V	0.24%
1 A	0.100 V	0.097 V	0.19%
1.5 A	0.150 V	0.145 V	0.33%
2 A	0.200 V	0.193 V	0.28%

表 9. Observation for Shunt-Based Current Sensing (continued)

INPUT CURRENT AT 50 Hz	INA240 EXPECTED OUTPUT	INA240 MEASURED OUTPUT	OUTPUT ERROR (%)
2.5 A	0.250 V	0.242 V	0.33%
3 A	0.300 V	0.290 V	0.26%
4 A	0.400 V	0.387 V	0.30%
5 A	0.500 V	0.484 V	0.29%
6 A	0.600 V	0.580 V	0.33%
7 A	0.700 V	0.677 V	0.26%
8 A	0.800 V	0.774 V	0.26%
9 A	0.900 V	0.871 V	0.24%
10 A	1.000 V	0.968 V	0.24%
11 A	1.100 V	1.064 V	0.24%

The maximum error in the sensor output is 0.33% and minimum error is 0.19%. The variation of error in sensor output is 0.14% for (0.5 A–11 A) current range.

表 10. Observation for Hall Effect-Based Current Sensing

INPUT CURRENT AT 50 Hz	HALL EFFECT SENSOR EXPECTED OUTPUT	HALL EFFECT SENSOR MEASURED OUTPUT	OUTPUT ERROR (%)
0.5 A	0.0208 V	0.0209 V	0.53%
1 A	0.0417 V	0.0419 V	0.63%
1.5 A	0.0625 V	0.0629 V	0.64%
2 A	0.0833 V	0.0839 V	0.68%
2.5 A	0.1042 V	0.1048 V	0.60%
3 A	0.1250 V	0.1257 V	0.58%
4 A	0.1667 V	0.1676 V	0.54%
5 A	0.2083 V	0.2095 V	0.56%
6 A	0.2500 V	0.2514 V	0.54%
7 A	0.2917 V	0.2934 V	0.58%
8 A	0.3333 V	0.3352 V	0.55%
9 A	0.3750 V	0.3771 V	0.56%
10 A	0.4167 V	0.4190 V	0.55%
11 A	0.4583 V	0.4609 V	0.56%

The maximum error in the sensor output is 0.68% and minimum error is 0.53%.

The variation of error in sensor output is 0.15% for (0.5 A–11 A) current range.

Shunt-based current sensing has lower error variation of 0.14% for AC current input range (0.5 A–11 A) at 50 Hz whereas Hall effect based current sensing has a higher error variation of 0.15%.

表 11 and 表 12 show the test data observed at 60 Hz for 0.5 A to 11 A RMS input current range:

表 11. Observation for Shunt-Based Current Sensing

INPUT CURRENT AT 60 Hz	INA240 EXPECTED OUTPUT	INA240 MEASURED OUTPUT	OUTPUT ERROR (%)
0.5 A	0.050 V	0.048 V	0.21%
1 A	0.100 V	0.097 V	0.24%
2 A	0.200 V	0.193 V	0.28%
6 A	0.600 V	0.580 V	0.27%
11 A	1.100 V	1.065 V	0.22%

The calibration factor at output is 3.

The maximum error in the sensor output is 0.28% and the minimum error is 0.21%. The variation of error in the sensor output is 0.07% for (0.5 A–11 A) current range.

表 12. Observation for Hall Effect-Based Current Sensing

INPUT CURRENT AT 60 Hz	HALL EFFECT SENSOR EXPECTED OUTPUT	HALL EFFECT SENSOR MEASURED OUTPUT	OUTPUT ERROR (%)
0.5 A	0.021 V	0.021 V	0.62%
1 A	0.042 V	0.042 V	0.51%
2 A	0.083 V	0.084 V	0.52%
6 A	0.250 V	0.251 V	0.42%
11 A	0.458 V	0.460 V	0.44%

The maximum error in the sensor output is 0.62% and the minimum error is 0.44%. The variation of error in the sensor output is 0.18% for (0.5 A–11 A) current range.

Shunt-based current sensing has a lower error variation of 0.07% for AC current input range (0.5 A–11 A) at 60 Hz; whereas Hall effect-based current sensing has a higher error variation of 0.18%.

表 13 and 表 14 show the test data observed at 400 Hz for 0.5 A to 11 A RMS input current range:

表 13. Observation for Shunt-Based Current Sensing

INPUT CURRENT AT 400 Hz	INA240 EXPECTED OUTPUT	INA240 MEASURED OUTPUT	OUTPUT ERROR (%)
0.5 A	0.050 V	0.048 V	0.16%
1 A	0.100 V	0.097 V	0.20%
2 A	0.200 V	0.193 V	0.26%
6 A	0.600 V	0.581 V	0.25%
11 A	1.100 V	1.065 V	0.20%

The maximum error in the sensor output is 0.26% and the minimum error is –0.16%. The variation of error in the sensor output is 0.10% for the (0.5 A–11 A) current range

表 14. Observation for Hall Effect-Based Current Sensing

INPUT CURRENT AT 400 Hz	HALL EFFECT SENSOR EXPECTED OUTPUT	HALL EFFECT SENSOR MEASURED OUTPUT	OUTPUT ERROR (%)
0.5 A	0.021 V	0.021	0.848%
1 A	0.042 V	0.042	0.754%
2 A	0.083 V	0.084	0.748%
6 A	0.250 V	0.252	0.619%
11 A	0.458 V	0.461	0.617%

The maximum error in the sensor output is 0.848% and the minimum error is 0.617%. The variation of error in the sensor output is 0.23% for (0.5 A–11 A) current range.

Shunt-based current sensing has a lower error variation of 0.10% for AC current input range (0.5 A–11 A) at 400 Hz; whereas the Hall effect-based current sensing has a higher error variation of 0.23%.

3.2.4.1 Summary of AC Current Measurement Performance Testing

表 15. AC Current Measurement Performance Testing

FREQUENCY	INPUT CURRENT RANGE	VARIATION IN ERROR FOR SHUNT-BASED SENSING (%)	VARIATION IN ERROR FOR HALL EFFECT BASED SENSING
50 Hz	0.5 A–11 A	0.14%	0.15%
60 Hz	0.5 A–11 A	0.07%	0.18%
400 Hz	0.5 A–11 A	0.10%	0.23%

Shunt-based current sensing has a lower error for AC current input range 0.5 A, 11 A at 50 Hz, 60 Hz and 400 Hz than Hall effect-based current sensing.

3.2.5 Fault Detection Performance Testing

3.2.5.1 Comparator Response Time

This section provides details of fault detection performance testing. A function generator was used to provide an input square wave to the comparator and the response time of the comparators was observed using an oscilloscope.

表 16. Comparator Response Time

COMPARATOR	PULLUP RESISTOR VALUE	DELAY IN OVERCURRENT DETECTION	DELAY IN UNDERCURRENT DETECTION
LM393A	3.3 kΩ	1.24 µs	208 ns
LMV393	3.3 kΩ	148 ns	136 ns
TLC372	3.3 kΩ	500 ns	148 ns
TLV3202	Internal pullup network	48 ns	56 ns

The TIDA-01598 uses an LMV393 comparator for fault detection as it shows a low delay in overcurrent and undercurrent detection at lower cost. The delay for overcurrent detection is 148 ns and the delay for undercurrent detection is 136 ns.

The resistance value of the pullup resistors can be lowered to reduce the rise time delay shown by the comparator. 表 17 shows the variation in delay of the LM393 comparator output with a change in the pullup resistor.

表 17. LM393 Comparator Output Delay Variation

COMPARATOR	PULLUP RESISTOR VALUE	DELAY IN RISE TIME
LM393A	3.3 kΩ	1.24 µs
LM393A	2.7 kΩ	1.20 µs

3.2.5.2 System Fault Response Time

A function generator was used to provide an input square wave to the input of INA240 and the response time was observed using an oscilloscope. This will include any delay inherent in the INA240, providing a full system response time. The delay between a high input transition and the active-low state of OUT_A is the system overcurrent detection delay. Undercurrent response time is measured by the delay between a low input transition and the active-low output of OUT_B. These delays are illustrated in 図 13 and 図 14.

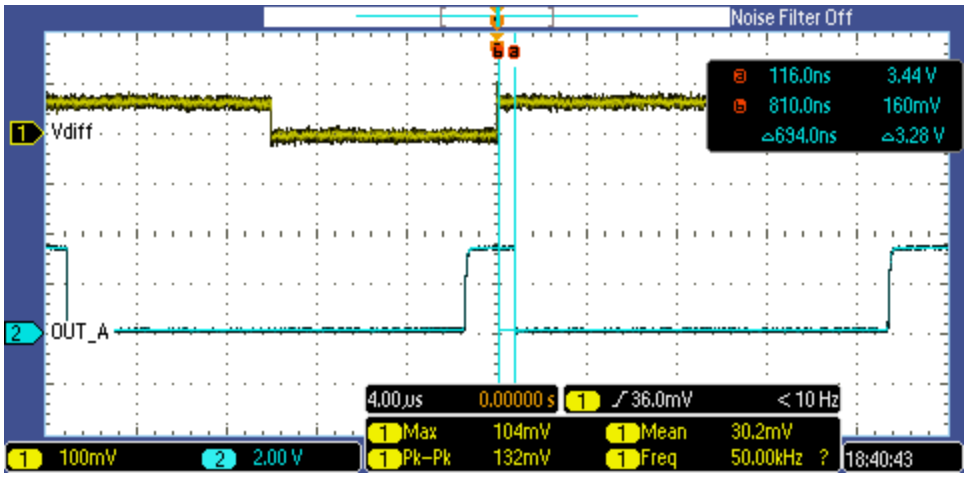

図 13. Overcurrent Detection Delay at 50 kHz

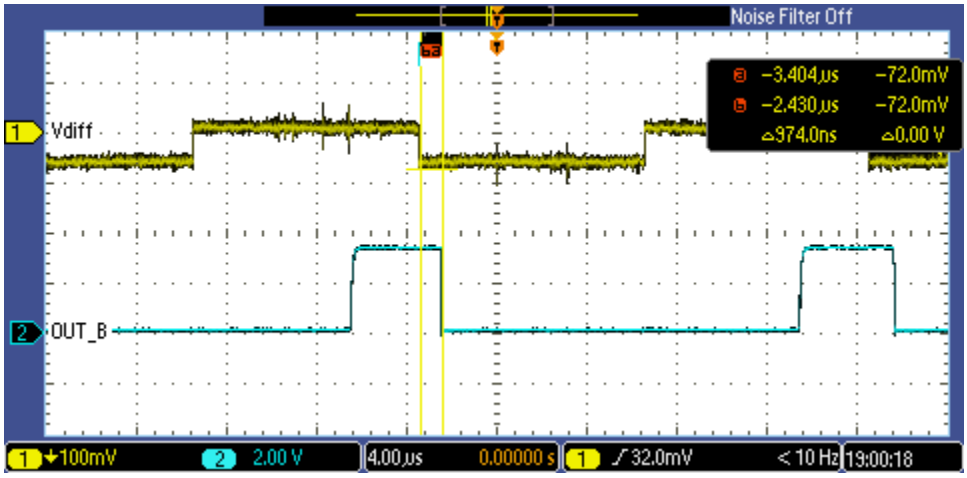

図 14. Undercurrent Detection Delay at 50 kHz

表 18. Overcurrent and Undercurrent Fault System Delay

COMPARATOR	PULLUP RESISTOR	INPUT FREQUENCY	OVERCURRENT DELAY	UNDERCURRENT DELAY
LMV393	3.3 kΩ	50 kHz	900 ns	990 ns
		100 kHz	780 ns	1 µs
		400 kHz	880 ns	806 ns
	2.7 kΩ	50 kHz	894 ns	874 ns
		100 kHz	708 ns	714 ns
		400 kHz	894 ns	866 ns

3.2.6 Test Results Summary

表 19 summarizes the test and observations for the TIDA-01598 TI design.

表 19. Test Results Summary

TEST	OBSERVATION
DC current measurement performance	OK
AC current measurement performance	OK
LDO output	OK
Reference voltage output	OK
Scaling amplifier	OK
Fault detection	OK

4 Design Files

4.1 Schematics

To download the schematics, see the design files at TIDA-01598.

4.2 Bill of Materials

To download the bill of materials (BOM), see the design files at TIDA-01598.

4.3 PCB Layout Recommendations

4.3.1 Layout Prints

To download the layer plots, see the design files at TIDA-01598.

4.4 Altium Project

To download the Altium Designer® project files, see the design files at TIDA-01598.

4.5 Gerber Files

To download the Gerber files, see the design files at TIDA-01598.

4.6 Assembly Drawings

To download the assembly drawings, see the design files at TIDA-01598.

5 Related Documentation

1. Texas Instruments, *INA240 High- and Low-Side, Bidirectional, Zero-Drift, Current-Sense Amplifier With Enhanced PWM Rejection Data Sheet*
2. Texas Instruments, *LMV33x-N / LMV393-N General-Purpose, Low-Voltage, Tiny Pack Comparators Data Sheet*
3. Texas Instruments, *TLV431x Low-Voltage Adjustable Precision Shunt Regulator Data Sheet*
4. Texas Instruments, *OPAx350 High-Speed, Single-Supply, Rail-to-Rail Operational Amplifiers MicroAmplifier Series Data Sheet*
5. Texas Instruments, *SN74LVC1G17 Single Schmitt-Trigger Buffer Data Sheet*
6. Texas Instruments, *TPS717 Low-Noise, High-Bandwidth PSRR, Low-Dropout, 150-mA Linear Regulator Data Sheet*

7. Texas Instruments, *LP2985 150-mA Low-noise Low-dropout Regulator With Shutdown Data Sheet*
8. Texas Instruments, *TLV760 100-mA, 30-V, Fixed-Output, Linear-Voltage Regulator Data Sheet*

5.1 Trademarks

6 About the Author

Vaibhavi Shanbhag is a project trainee in the Industrial Systems team at Texas Instruments where she is responsible for developing reference design solutions with a focus on Grid Infrastructure. Vaibhavi is a final-year student pursuing a Bachelor of Engineering (B.E. Hons.) in Electrical and Electronics Engineering from Birla Institute of Technology & Sciences (BITS), Pilani K.K.Birla Goa Campus.

BART BASILE is a systems architect in the Grid Infrastructure Solutions Team at Texas Instruments, where he focuses on renewable energy and EV infrastructure. Bart works across multiple product families and technologies to leverage the best solutions possible for system level application design. Bart received his bachelors of science in electronic engineering from Texas A&M University.

TIの設計情報およびリソースに関する重要な注意事項

Texas Instruments Incorporated ("TI")の技術、アプリケーションその他設計に関する助言、サービスまたは情報は、TI製品を組み込んだアプリケーションを開発する設計者に役立つことを目的として提供するものです。これにはリファレンス設計や、評価モジュールに関係する資料が含まれますが、これらに限られません。以下、これらを総称して「TIリソース」と呼びます。いかなる方法であっても、TIリソースのいずれかをダウンロード、アクセス、または使用した場合、お客様(個人、または会社を代表している場合にはお客様の会社)は、これらのリソースをここに記載された目的にのみ使用し、この注意事項の条項に従うことに合意したものとします。

TIによるTIリソースの提供は、TI製品に対する該当の発行済み保証事項または免責事項を拡張またはいかなる形でも変更するものではなく、これらのTIリソースを提供することによって、TIにはいかなる追加義務も責任も発生しないものとします。TIは、自社のTIリソースに訂正、拡張、改良、およびその他の変更を加える権利を留保します。

お客様は、自らのアプリケーションの設計において、ご自身が独自に分析、評価、判断を行う責任がお客様にあり、お客様のアプリケーション(および、お客様のアプリケーションに使用されるすべてのTI製品)の安全性、および該当するすべての規制、法、その他適用される要件への遵守を保証するすべての責任をお客様のみが負うことを理解し、合意するものとします。お客様は、自身のアプリケーションに関して、(1) 故障による危険な結果を予測し、(2) 障害とその結果を監視し、および、(3) 損害を引き起こす障害の可能性を減らし、適切な対策を行う目的での、安全策を開発し実装するために必要な、すべての技術を保持していることを表明するものとします。お客様は、TI製品を含むアプリケーションを使用または配布する前に、それらのアプリケーション、およびアプリケーションに使用されているTI製品の機能性を完全にテストすることに合意するものとします。TIは、特定のTIリソース用に発行されたドキュメントで明示的に記載されているもの以外のテストを実行していません。

お客様は、個別のTIリソースにつき、当該TIリソースに記載されているTI製品を含むアプリケーションの開発に関連する目的でのみ、使用、コピー、変更することが許可されています。明示的または黙示的を問わず、禁反言の法理その他どのような理由でも、他のTIの知的所有権に対するその他のライセンスは付与されません。また、TIまたは他のいかなる第三者のテクノロジまたは知的所有権についても、いかなるライセンスも付与されるものではありません。付与されないものには、TI製品またはサービスが使用される組み合わせ、機械、プロセスに関連する特許権、著作権、回路配置利用権、その他の知的所有権が含まれますが、これらに限られません。第三者の製品やサービスに関する、またはそれらを参照する情報は、そのような製品またはサービスを利用するライセンスを構成するものではなく、それらに対する保証または推奨を意味するものでもありません。TIリソースを使用するため、第三者の特許または他の知的所有権に基づく第三者からのライセンス、もしくは、TIの特許または他の知的所有権に基づくTIからのライセンスが必要な場合があります。

TIのリソースは、それに含まれるあらゆる欠陥も含めて、「現状のまま」提供されます。TIは、TIリソースまたはその仕様に関して、明示的か暗黙的かにかかわらず、他のいかなる保証または表明も行いません。これには、正確性または完全性、権原、続発性の障害に関する保証、および商品性、特定目的への適合性、第三者の知的所有権の非侵害に対する黙示の保証が含まれますが、これらに限られません。

TIは、いかなる苦情に対しても、お客様への弁護または補償を行う義務はなく、行わないものとします。これには、任意の製品の組み合わせに関連する、またはそれらに基づく侵害の請求も含まれますが、これらに限られず、またその事実についてTIリソースまたは他の場所に記載されているか否かを問わないものとします。いかなる場合も、TIリソースまたはその使用に関連して、またはそれらにより発生した、実際的、直接的、特別、付随的、間接的、懲罰的、偶発的、または、結果的な損害について、そのような損害の可能性についてTIが知らされていたかどうかにかかわらず、TIは責任を負わないものとします。

お客様は、この注意事項の条件および条項に従わなかったために発生した、いかなる損害、コスト、損失、責任からも、TIおよびその代表者を完全に免責するものとします。

この注意事項はTIリソースに適用されます。特定の種類の資料、TI製品、およびサービスの使用および購入については、追加条項が適用されます。これには、半導体製品(http://www.ti.com/sc/docs/stdterms.htm)、評価モジュール、およびサンプル(http://www.ti.com/sc/docs/sampterms.htm)についてのTIの標準条項が含まれますが、これらに限られません。